UNIVERSIDAD DISTRITAL
FRANCISCO JOSÉ DE CALDAS

Ingeniería

https://revistas.udistrital.edu.co/index.php/reving/issue/view/1350

DOI: https://doi.org/10.14483/23448393.e22588



Research

Characterization and Zoning of Iron Deposits Using Geophysical Methods: Magnetometry and Geoelectrics in a Rural Area of Paipa, Colombia

Caracterización y zonificación de depósitos de hierro mediante métodos geofísicos: magnetometría y geoeléctrica en una zona rural de Paipa, Colombia

Luis Miguel Fernández Ricardo[1], Alejandro Herrera Tovar[2] , and Robinson Quintana Puentes[3] *

[1]Unidad Administrativa Especial de Catastro de Bogotá (Bogotá, Colombia)
[2]MHC Ingeniería y construcción de obras civiles (Bogotá, Colombia)
[3]Universidad Distrital Francisco José de Caldas (Bogotá, Colombia),

Abstract

Context: This study presents the results of an analysis of magnetic and geoelectric data collected during a multiphase geophysical survey conducted in 2015 in the rural area of the municipality of Paipa, Boyacá, Colombia.
Method: Based on published studies and nearby geological outcrops where iron ore minerals such as goethite, hematite, and pyrite have been documented, the acquired geophysical data were interpreted.
Results: A 2D geological-geophysical model of the iron-associated deposits was obtained.
Conclusions: Evaluating the presence of these minerals and determining the susceptibility of the surrounding natural ecosystems and of surface and groundwater bodies detected with these techniques provide an additional technical tool for future mining exploitation licensing.

Keywords: geological-geophysical model, geophysics, magnetic anomaly, prospecting, resistivity.

Article history

Received:
October 16th, 2024

Modified:
April 17th, 2026

Accepted:
June 11th, 2026

Ing, vol. 31, no. 2, 2026, e22588

©The authors; reproduction right holder Universidad Distrital Francisco José de Caldas.

CC BY NC SA

* Correspondence: rquintanap@udistrital.edu.co

Resumen

Contexto: Este estudio presenta los resultados del análisis de los datos magnéticos y geoeléctricos recolectados en una campaña multifase de adquisición geofísica llevada a cabo en 2015 en la zona rural del municipio de Paipa, Boyacá, Colombia.

Método: Con base en estudios publicados y en afloramientos geológicos cercanos donde se ha documentado la presencia de minerales mena del hierro, como la goethita, la hematita y la pirita, se interpretaron los datos geofísicos adquiridos.

Resultados: Se obtuvo un modelo geofísico-geológico 2D de los depósitos asociados al hierro.

Conclusiones: Al evaluar la presencia de este tipo de minerales y al determinar la susceptibilidad sobre los ecosistemas naturales circundantes o cuerpos de agua superficiales y subterráneos detectados mediante las técnicas empleadas proporciona una herramienta técnica adicional para futuros procesos de licenciamiento de explotación minera.

***Palabras clave*:** modelo geológico-geofísico, geofísica, anomalía magnética, prospección, resistividad.

Contents

1. Introduction 3

2. Methodology 3

2.1. Study Zone 3
2.2. Magnetic Data Acquisition 7
2.3. Geoelectric Profiles 8
2.4. Data Processing 8

3. Results and Discussion 10

4. Conclusions 16

5. Acknowledgements 17

6. Author contributions 17

7. Funding 17

8. Data availability 17

9. Conflict of interest 17

10. Use of artificial intelligence 17

References 17

Authors and biographies 19

1. Introduction

Iron ore mining is crucial for steel production and infrastructure development in Colombian cities. To be sustainable, however, it must meet current needs without compromising those of future generations, and it must be accompanied by sound environmental management. Improved planning of mining operations stems from knowledge of the subsurface gained through exploration. The Colombian National Mining Agency (ANM) has published a document outlining the exploration phases and the work plan (Programa de Trabajos y Obras, PTO), point 4 of which addresses "Location, calculation, and characteristics of the reserves to be exploited during the project's development" [1]. This highlights the importance of using methods to characterize iron ore reserves. Additionally, the ANM has published the Mining and Environmental Exploration Guide (*Guía Minero Ambiental de Explotación*), which offers guidance aimed at improving the planning and projection of mining activities during the exploitation phase. The guide incorporates best available techniques, best environmental practices, and circular economy principles, among other elements [2].

It has been observed that the lack of knowledge of natural and environmental elements, such as water bodies (lagoons, streams, rivers, and springs) associated with the geological structures of mineral deposits, is the main cause of their deterioration and impairment, which could be avoided if their existence, location, and extent were known. This work proposes the application of geophysical methods, in this case magnetometry and geoelectrics, for the possible detection and characterization of these elements, in addition to verifying the continuation of iron-associated mineral deposits in a specific area of Colombia [3].

A total magnetic intensity map, a reduced-to-the-pole map, an analytic signal map, a vertical first derivative map, and an upward continuation map were obtained [4]. Using electrical resistivity tomography, a series of apparent resistivity measurements were obtained with a specific four-electrode array and a constant electrode spacing [5].

2. Methodology

2.1. Study Zone

The study area is located in the municipality of Paipa, in the Sogamoso Valley, one of the most important inter-Andean valleys of the center-eastern Andean region of Colombia, in the northwest of the department of Boyacá, at an elevation of 2,525 m above mean sea level (a.m.s.l.). It lies approximately 184 km from Bogotá and 40 km from Tunja. The iron mine under study is located 17.7 km from the municipal seat of Paipa, in the Vargas village, where the monument commemorative the Battle of Pantano de Vargas stands.

The municipality of Paipa currently has more than 55 mining titles granted by the ANM for the exploitation of coal, pozzolana, sand, limestone, and, to a lesser extent, iron. Of these titles, 70% are subject to some type of environmental instrument, which is understandable given that many of the titles granted are located within environmental water-protection zones and protective forests, such as the Sochagota Lake Integrated Management District (*Distrito de Manejo Integrado,* DIM), established by Agreement 30% and Resolution 262 of September 9, 1986, issued by the Ministry of Agriculture. Mining activity in the area has had environmental effects: the surface and underground water bodies near the mining polygons have low quality indices, and mining has also contributed to the loss of vegetation cover [6] [7].

In this work, the lithology of an iron mine located in the municipality of Paipa, Boyacá, covering an approximate area of 12,585 m^2 (see Figure 1), was characterized geophysically. In the surrounding region, various studies using electrical methods, seismic refraction, and gamma logging have been carried out in sectors classified as mining exploration zones for deposits of iron, copper, emeralds, among others. In addition, several geological studies of the area and its surroundings report the petrographic characterization of iron occurrences in various villages of the department of Boyacá. These studies include the logging of stratigraphic columns of the outcropping formations and their relationship with the volcanic activity that occurred during the Neogene in the southern region of Paipa. The work area was selected based on accessibility, ease of logistical setup, cost considerations, and the existing geological background of the sector [8].

Rocks ranging in age from the Triassic to the Upper Tertiary crop out in the area, together with some Quaternary deposits. The Boyacá Fault is one of the regional structural features that separates two sets of sedimentary layers with distinct morphostructural features.

North of the fault, there are Jura-Triassic and marine Cretaceous deposits with extensive folds. South of the same fault, there Tertiary continental sediments, Upper Cretaceous marine sediments, and outcrops of andesitic volcanic rocks [9]. Figure 2 shows the geological units that crop out in the study area.

As reported in [9], the main outcropping unit in the sector is the Tilatá Formation, which has been affected by igneous bodies of magmatic origin and tectonic processes, giving rise to geological units of volcanic origin. These units were informally named the El Volador Tertiary Unit (Tuv) and the Paipa Volcanic Unit. The El Volador Tertiary Unit (Tuv) consists of two segments (upper and lower). The upper segment is divided into four levels, characterized as sequences of fine- to coarse-grained clayey sandstones, some of them white, with wavy laminations in the claystones and inverse grading in the sandstones.

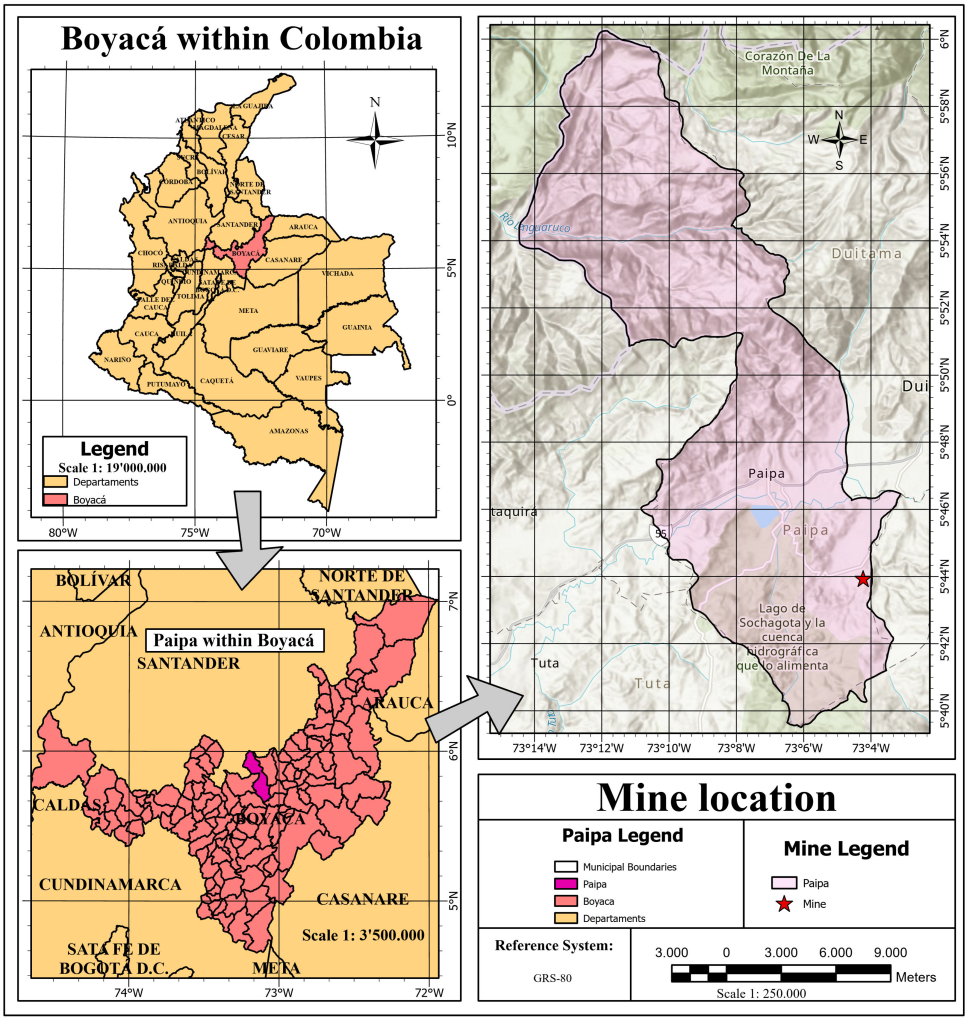


Figure 1. Location of the municipality of Paipa, Colombia.

Locally, the unit is affected by alteration processes such as silicification, which makes the conglomerate extremely hard, and injection of iron oxides, which replace the entire structure of the sandstones and generate an exploitable iron oxide deposit. According to verbal information from the administrator of the Vargas mine under study, the iron was between 70% and 80% [10].

The Paipa Volcanic Unit comprises two types of pyroclastic deposits: the Tobas del Guarrús and the Paipa Volcanic Unit. The Tobas del Guarrús (Figure 3) consists of two sequences, the first of which is described as a type of aerial projection tuff deposit, unrelated to the underlying unit and deposited on the El Volador Tertiary Unit (Tuv). It is a tabular deposit 30 m thick (gradating not observable). The second sequence is characterized as a pyroclastic-flow deposit unconformably overlying the Une, San Rafael, and Conejo formations, and the Tertiary unit [12].

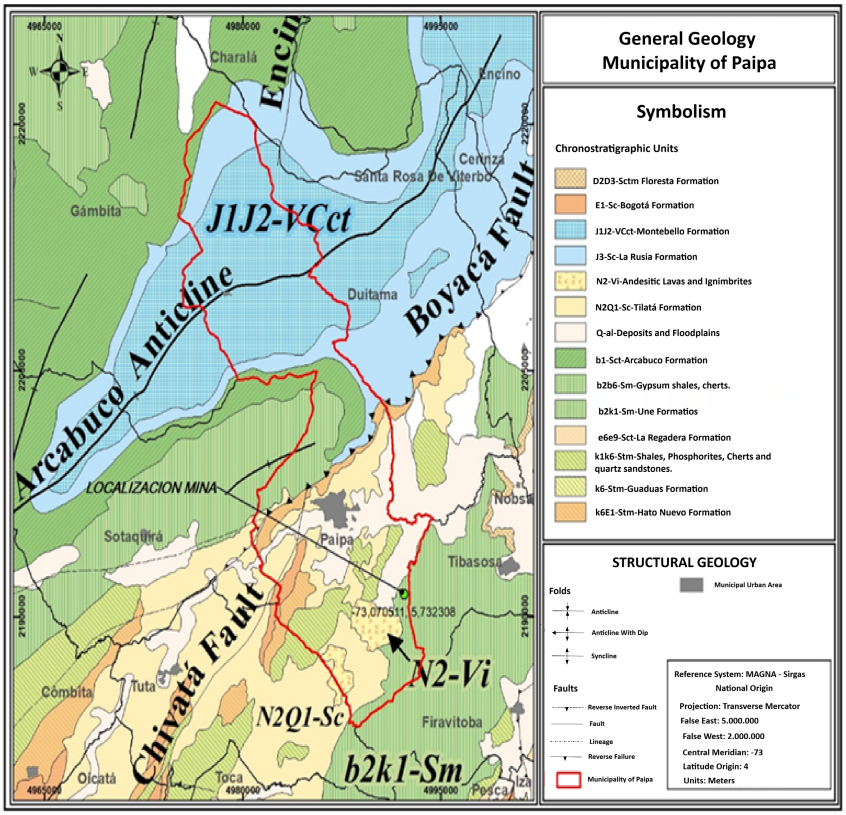


Figure 2. Regional geological framework, chronostratigraphic units. 1. Tilatá Formation (N2Q1-Sc), 2. Une Formation (b2k1-Sm), 3. Floresta Formation (D2D3-Sctm), 4. Bogota Formation (E1-Sc), 5. Guaduas Formation (K6-Stm), 6. Montebello Formation (J1J2-VCct), 7. La Rusia Formation (J3-Sc), 8. Arcabuco Formation (b1-Sct), 9. La Regadera Formation (e6e9-Sm), 10. Hato Nuevo Formation (k6E1), 11. Andesitic lava and ignimbrite deposits (N2-Vi), 12. Alluvial deposits and plains (Q-al). Source: Own elaboration based on information from the Geological Map of Colombia 2020, Colombian Geological Service [11].

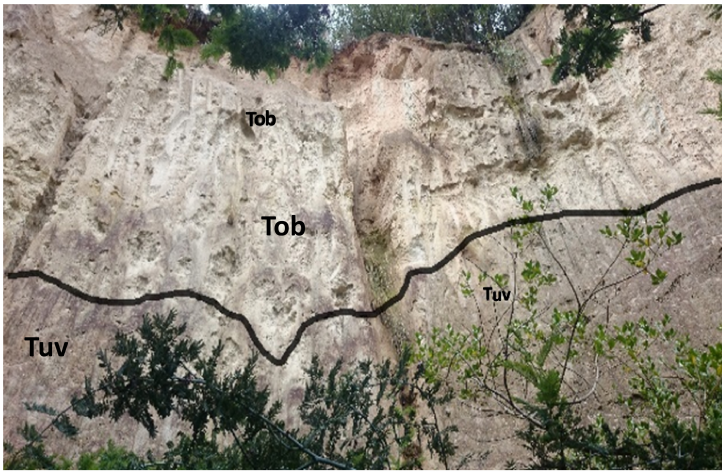


Figure 3. Segments 1 and 2 Tobas del Guarrús deposit (Tob), below the El Volador Tertiary Unit (Tuv).

A second deposit that makes up the Paipa Volcanic Unit, the Tephras of El Guarrús, overlies the Tobas del Guarrús (Figure 4) and is also divided into two sub-sequences. The first is a tabular segment with a maximum visible thickness of 3 m. It shows massive stratification, and its lithics include green schists, quartz arenites, and rhyolite fragments. The last sub-sequence is quite irregular in shape. The stratification of the laminae is flat and parallel. The intermediate layers present crossed stratification with layers of approximately 20 cm, and locally undulating non-parallel stratification is observed.



Figure 4. Segments 1 and 2, Tobas, Tefras of Guarrús deposit.

The approximate age of the proposed Tertiary El Volador unit is post-Paleocene to pre-Pliocene, a time interval characterized by the deposition of coarse sediments and by the deformation of Cretaceous-Tertiary sediments due to the strong movements of Andean orogeny. The age of the Paipa Volcanic Unit, on the other hand, is uncertain: the Instituto Colombiano de Energía Eléctrica (ICEL) reports an age of 2.5 Ma but provides no additional data. However, this unit unconformably overlies the El Volador Tertiary Unit, indicating that the latter is older; therefore, the Paipa Volcanic Unit could be dated as Pliocene or Pleistocene. Furthermore, the current geothermal activity in the area may correspond to the last phase of very recent major geothermal activity [12].

2.2. Magnetic Data Acquisition

Magnetometry: As a first step, a topographic survey was carried out to delimit the study area in addition to making a grid which had the objective of planning the acquisition of magnetometry data and providing confidence in the positioning of the acquisition points. The points were marked, and their coordinates were obtained and referenced to the MAGNA-SIRGAS coordinate system, Bogotá origin. Dual-frequency GPS equipment and differential positioning methods were used.

The magnetometric survey in the study area was carried out with a Geometrics G-856 proton precession magnetometer (base and mobile units), with a precision of 0.1 nT. The magnetometer consists of a cylindrical sensor mounted on a metal tube of approximately 2 m and a console from which the instrument is operated, and the field readings are displayed. Figure 5 shows the distribution of the points measured in the field with both the base and the mobile magnetometer.

2.3. Geoelectric Profiles

The analysis of the magnetic data made it possible to establish where the geoelectric data would be acquired. The length of the profiles was limited by topographic highs, ground cover, lineaments, domains, and magnetic anomalies. The distances between emitter-receiver electrode pairs were varied in multiples of a specific value, yielding a cross-section with measurements at various depths. The results are plotted on pseudo-sections of apparent resistivity, thus forming a two-dimensional mesh. A pseudo-section is a section with iso-resistivity curves that qualitatively reflect the spatial (2D) variation of apparent resistivity along the investigated profile. Profiles were placed on these sites to characterize the resistivity distribution of the units present in the area. Three profiles were laid out parallel to the direction of the formation strata, and a fourth profile was laid out perpendicular to them, crossing all three. The dipole-dipole arrangement was used, because it provides both vertical and horizontal resolution suited to the needs of the work, with an electrode spacing of 5 m. Measurements were made with an ABEM SAS 1000 Terrameter, which allows obtaining resistivity profiles with a dipole-dipole electrode configuration. Figure 5 shows the location of the geoelectric profiles relative to the previously measured magnetic points.

2.4. Data Processing

After the acquisition, the data were organized, refined, and processed with specialized software. Oasis montaj version 6.4.2 (2007) was used for the potential-field data, and RES2DINV inversion software, which uses a smoothness-constrained least-squares routine [13], was used to obtain the tomography, from which the true resistivities and the 2D model are derived. The magnetic data were corrected for diurnal drift, and a total magnetic field (TMF) map was obtained by minimum-curvature interpolation.

Several conventional filters were applied during processing, which made it possible to interpret the measurements and correlate them with the geology. In general, TMF and residual magnetic field (RMF) maps were obtained; the latter is also known as the magnetic anomaly map. The normal field (International Geomagnetic Reference Field, IGRF) and, in some cases, the regional field were subtracted from the total field to obtain the residual map. Fourier-transform filters were then applied to highlight the sources of the magnetic anomalies [14]. Reduction to the pole, which also places the anomalies vertically over the magnetic sources, was followed by inversion of the magnetic field to obtain 2D models of magnetic susceptibility. The inverse modeling software, GM-SYS [15], uses a Marquardt inversion algorithm. The anomalies are treated as polygonal bodies with different levels of magnetization, which allows 2D modeling.

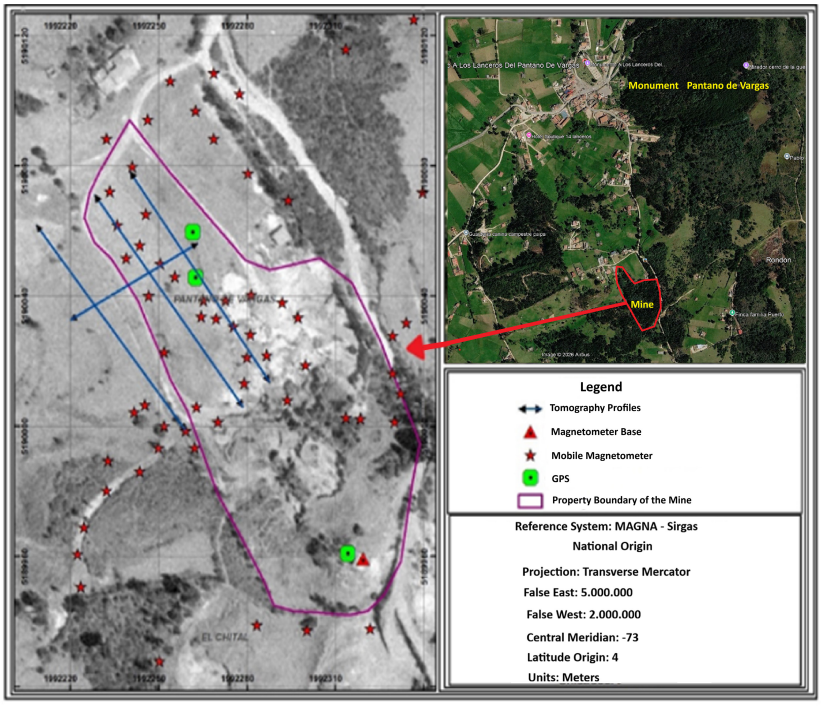


Figure 5. GPS location, magnetic sampling points and electrical profiles.

The model is done by construction of a 2D cross-section using several polygons with different geometries and magnetic susceptibilities, the latter obtained from measurements [16]. The starting values are real values associated with the minerals present in the area, ranging from -0.00211 to 0.0025 cgs for iron minerals such as pyrite, goethite, and hematite. The model is adjusted by modifying the shape, location, and characteristics of the polygons [17].

For the resistivity data, RES2DINV software was used [18], which allows inversions of the measured data to obtain the real resistivity distribution, commonly called a 2D resistivity tomography. This software has advanced modeling subroutines used to estimate apparent resistivity values. The software follows a structured, iterative mathematical sequence: it first imports and formats the data, then automatically divides the subsurface into a model consisting of blocks or cells. The size of these cells is typically linked to the spacing between the electrodes.

Using the finite element or finite difference method, RES2DINV calculates the theoretical apparent resistivity that this block model would produce if measured at the surface. It then compares the values measured in the field with these theoretically calculated values; this discrepancy is expressed as the RMS error. Finally, the software adjusts the resistivity values of the subsurface blocks and repeats the calculation (through iterations) until the RMS error stabilizes or falls below an acceptable threshold. We use the "Select Robust Inversion" method for standard least-squares optimization. This tends to generate "smooth" or blurred transition models. This workflow was also used by another author [19].

3. Results and Discussion

Below are the maps derived from the magnetometric information, together with a brief interpretation of each map, the tomography, and the models derived from data processing. First, the total magnetic field map was obtained, which shows the values of the readings made in the field. Maximum field values of approximately 31,360 nT (nanotesla) and minimum values of approximately 31,200 nT are observed. This variation makes it possible to visualize field anomalies produced by sources in the shallow crust, since the main field (produced by the Earth's core) varies in intensity by approximately 1,000 nT per 1,000 km. The map allows direct observation of magnetic highs (red) where the total field is assumed to be more intense owing to the influence of minerals with high magnetic susceptibility. Figure 6 shows the total field map.

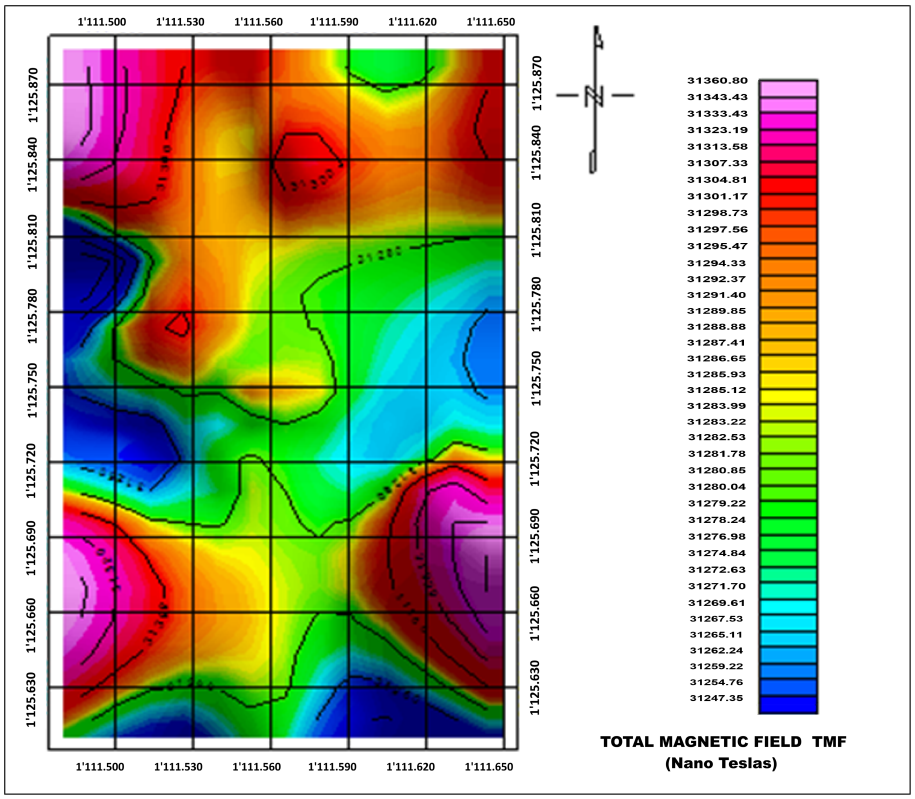


Figure 6. Total magnetic field map (TMF).

Next, the residual anomaly map was obtained. A Butterworth filter was used, and the radial power spectrum was applied to find the cutoff spatial frequency parameters and the he filter degree, which made it possible to separate the residual anomalies (high-pass range) from the regional anomalies (low-pass range). Figure 7 shows the residual anomaly map after applying the filter to the total field map.

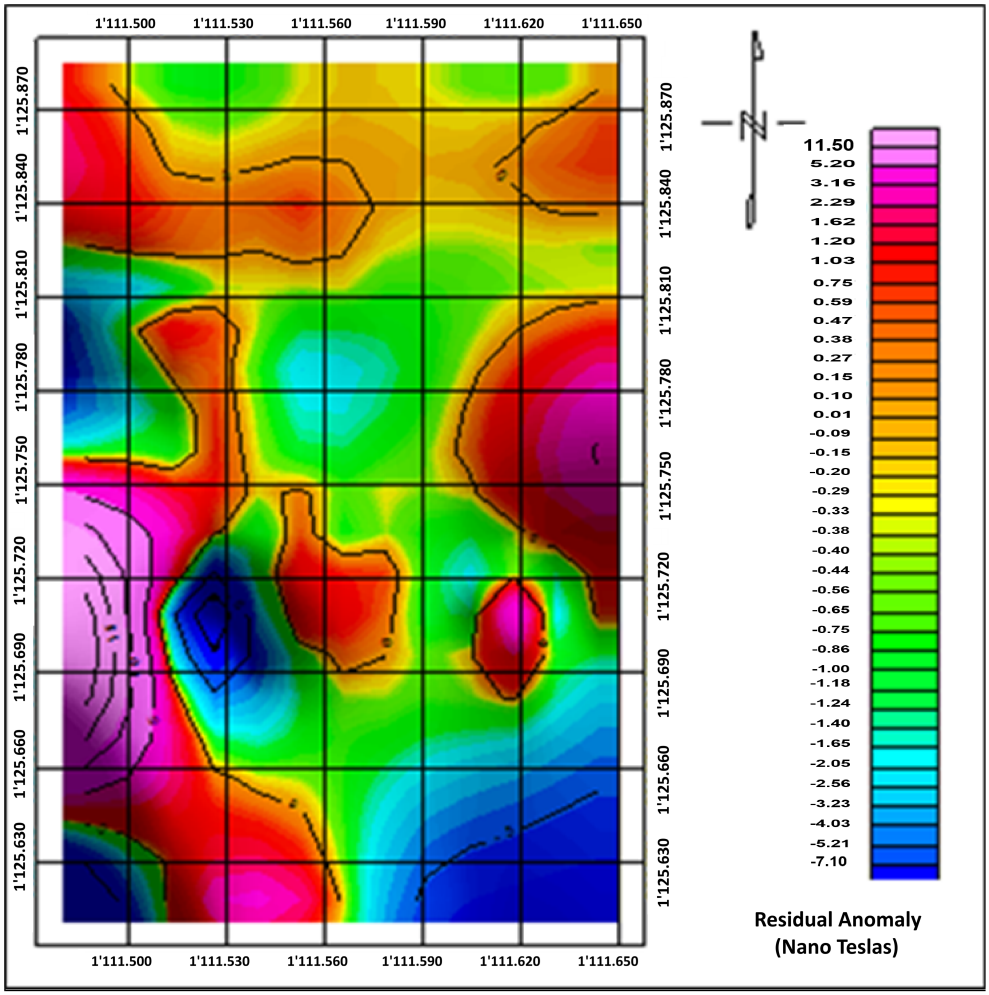


Figure 7. Map of residual anomalies (RA).

Total Field Magnetic Anomaly values in the study area range from -7 nT to 11 nT. Figure 7 shows the long-wavelength magnetic anomalies to the west and east. According to what was inferred from petrographic studies of the rocks that crop out in this sector [10], this distribution of magnetic anomalies could be related iron mineral formations such as goethite, hematite, and pyrite.

The residual anomaly map was used in the subsequent processes because shallow anomalies are of greatest interest in this work. Next, the reduction to the pole was applied to the residual anomaly map (Figure 8) to eliminate its bipolar character and convert it into unipolar, simplifying the shapes of the magnetic anomalies.

The usefulness of the filter lies in the fact that it places the magnetic residual anomalies at their true position, vertically above their magnetic sources. Compared with the residual anomaly map, the map reduced to the pole shows the bodies as continuous features. This map is displayed as a contour map of

the anomalies, although interpretation is often made on profiles. As all contoured maps, closely spaced lines represent a steep gradient (a rapid change in values), whereas widely spaced lines exhibit a shallow gradient (a slow change in values). This technique is employed to plot the magnetic data as a color image (red=high positive, blue=low negative, and the shades in between representing the values in between). The positive negative anomaly separates two positive anomalies to the east and the west. The negative anomalies correspond to normally magnetized rocks. The positive anomaly occurs in a demagnetized zone corresponding to the heat source of silicic origin. This provides some evidence of a heat source to the surface at a temperature above the Curie point of magnetite (above 575 °C) close to the surface. This gives an image that is easy to read, such as that shown in Figure 8. It is useful to know that magnetite is found in greater concentrations in igneous and metamorphic rocks. Magnetite can also be weathered or leached from rocks and re-deposited in other locations [20].

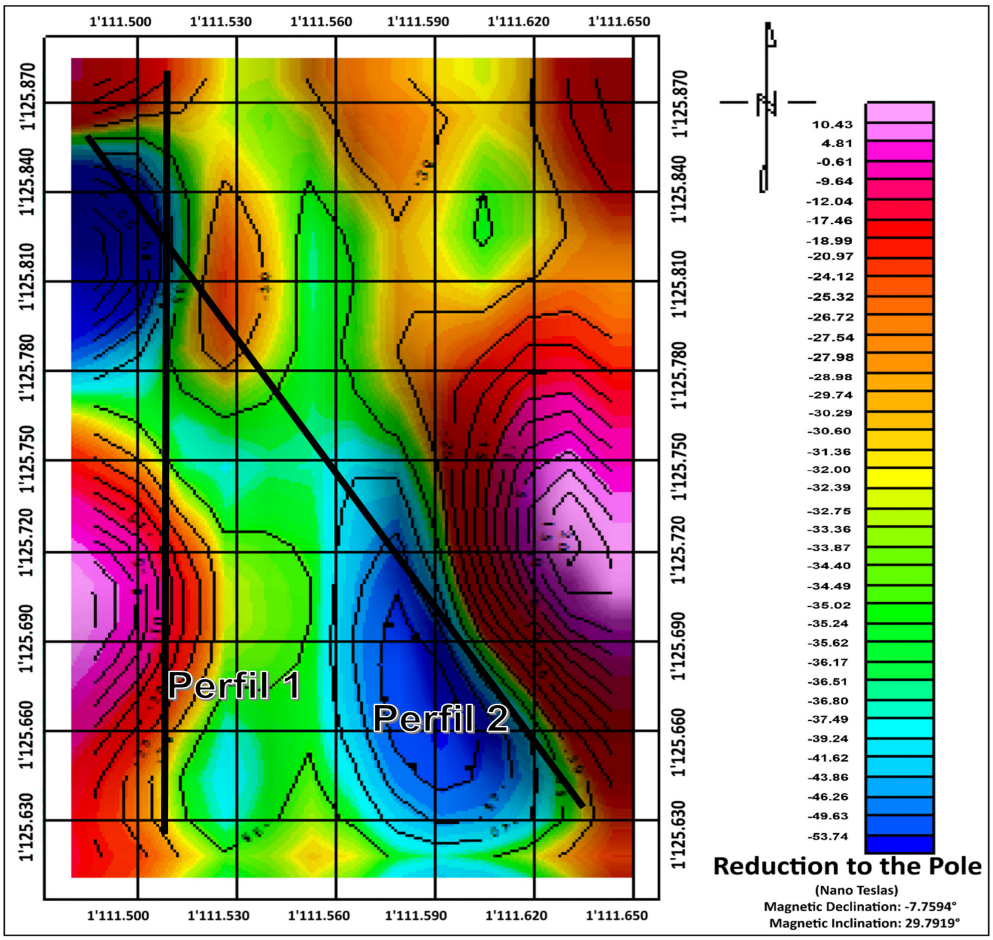


Figure 8. Map of anomalies with reduction to pole. Profiles drawn for 2D modeling are shown in black.

Since this last map shows the anomalies in their real position and with their associated magnetic intensity, 2D modeling was carried out on the two profiles located on this map. 2D modeling allows analysis of the sources that generate the anomalies. Magnetic inversion is affected by the non-uniqueness

problem; that is, it does not have a single solution, and several different solutions can produce the same fit between the calculated and observed fields. To narrow down the model solutions, we start from the geological information analyzed and from the information inferred from the filters applied to the magnetometry data. The basement depth was estimated from sediment thicknesses of around 650 m calculated by other author [21]. The profiles are shown in Figures 9 and 10.

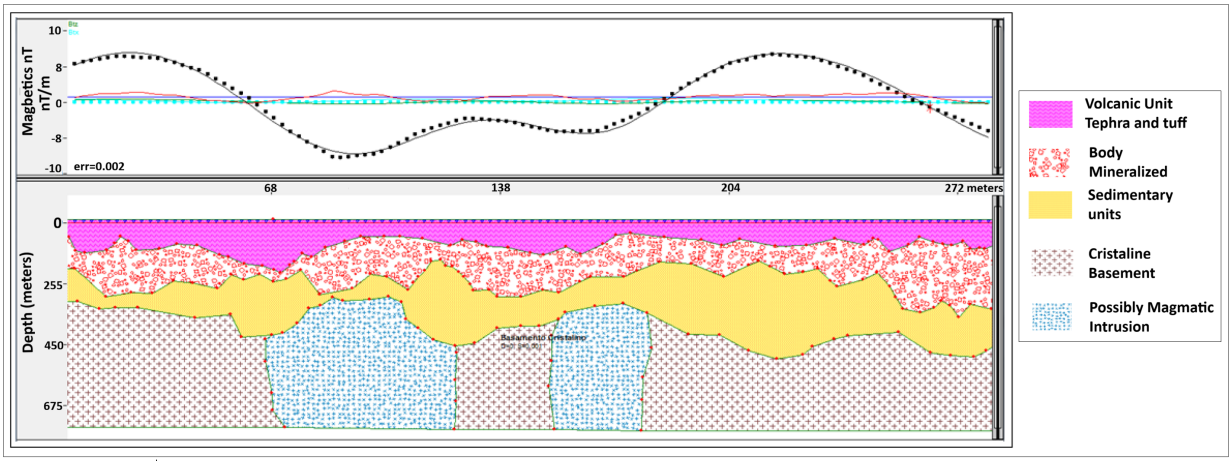


Figure 9. (a) Observed and calculated fields (solid black line: calculated field; dotted black line: observed field). (b) Geological–geophysical model, Profile 1.

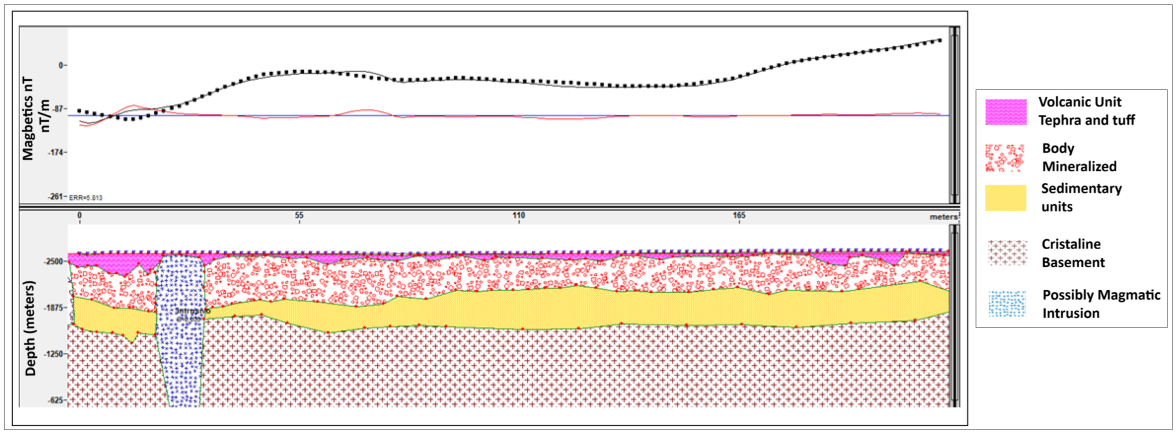


Figure 10. (a) Observed and calculated fields (solid black line: calculated field; dotted black line: observed field). (b) Geological–geophysical model, Profile 2.

The inversion process matches the theoretical magnetic anomaly produced by the bodies added to the model to the observed anomaly, whose intensity values are taken from the residual anomaly map reduced to the pole.

For this procedure, the GM-SYS program was used. Profile 1 is approximately 300 m long and runs in the North-East and North-South directions, respectively. It shows the influence of layers of volcanic

origin (shallow layer) and of iron oxidation (in red). The influence of the basement (approximate depth) and of intrusive bodies with high susceptibility is also shown at depth.

Profile 2 is 250 m long and runs in the N–E direction. It shows the influence of the body that contains the iron mineralization, which crops out along a large part of the profile. The light-yellow layer shows the sedimentary facies, mainly those of the Tilatá Formation, which have a very low susceptibility (sandstones, quartz arenites, quartz shales, etc.).

Finally, the geoelectric data were processed. The final models correspond to the geological–geophysical models, which allow inference of the position, length, and layout of the deposits or mineralized bodies of economic interest. For the two-dimensional inversion, the data taken in the field are digitized in a file with the extension .DAT so that the software can read and process them. The data file is read by the program, and an inversion is then run with the program's default parameters. These are generally standard and work well for data of acceptable quality, that is, data without a high level of noise, with good electrode sensitivity and acceptable resistivity ranges. Before processing, a cleaning procedure is carried out to eliminate outliers that may affect the inversion. This processing was done for the four profiles measured in the field.

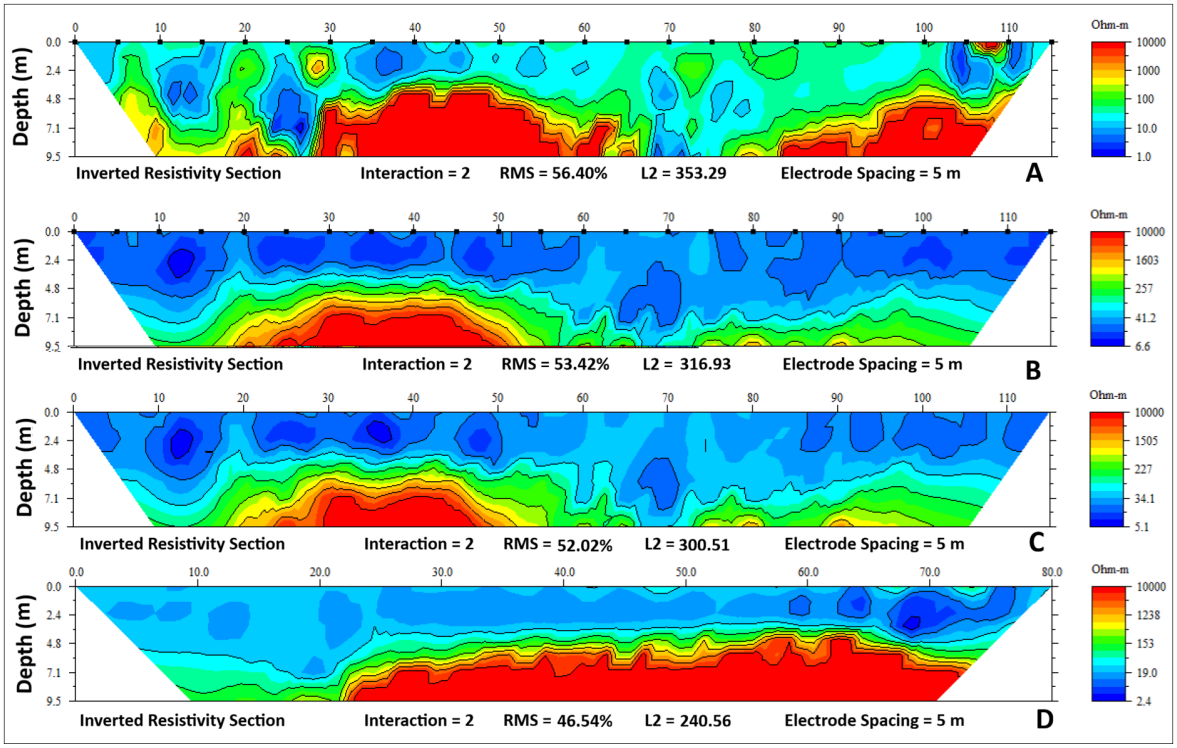


Figure 11. Resistivity tomography. True resistivity distribution: (a) Profile 1 (110 m), (b) Profile 2 (110 m), (c) Profile 3 (110 meters), (d) Profile 4 (transverse).

Once the 2D models were obtained, the different processing parameters, such as the inversion method or the value of the damping factor, were varied to improve each result and to reduce the misfit between the observed values and the calculated values. The error between the measured and calculated resistivity values was controlled, while maintaining morphologies that were generally constant and adequate in geological terms. The damping factor chosen was 1; according to Loke and Barker [13], the smaller this factor, the better the resolution of the deconvoluted model [22]. The tomographies were generated with RES2DINV software, but for presentation purposes the EarthImager 2D software (Advanced Geosciences Inc.) was used, which has its own adjustments or inversion parameters. This software also accepts the .DAT format for RES2DINV [13]. EarthImager 2D solves the direct model by means of Cholesky decomposition within a conjugate-gradient scheme (Figure 11).

The resistivity values and domains established in Table I (resistivity being the opposition of rocks to the passage of electric current, expressed in Ω·m) can be correlated with the previously studied local geology. The values very close to the surface, between 0-50 Ω·m, are considered to correspond to the residual soil of the sector and to a layer of altered, very poorly permeable volcanic tephras. Domain 2 comprises two ranges of resistivity values, one between 60-100 Ω·m and 150-250 Ω·m. In Domain 3, much higher resistivity values are found, between 600 and 800 Ω·m, rising to 900 and 1200 Ω·m; this last layer is interpreted as moderately altered, little fractured, and moderately permeable deposits of pyroclastic origin (volcanic tuffs).

Table I. Resistivity intervals obtained

Domain	Resistivity value (Ω·m)
1	0-5
2	60-100
	150-250
3	300-500
	600-800
	900-1200

According to the geological analysis of the area and the model created from the magnetic data, the lithology is of volcanic origin. Iron-associated minerals are found at low resistivity values (0–50 Ω·m) and, according to the tomography, are distributed in the shallow part of the formations, above the volcanic deposits and below the residual soil.

Correlating the results of the magnetic, geoelectric, and geological analyses allows the development of one of the most accurate models of the rock formations associated with iron mineralization in the area. This improves the planning and forecasting of mining activities during the exploitation phase.

It could also help avoid the removal or undermining of subsurface areas that contain underground or surface water bodies susceptible to contamination or that supply drinking water to nearby communities. Likewise, it makes it possible to characterize the residual soil cover and estimate its thickness for future vegetation recovery. Although no phreatic layers were detected in this work, the geoelectric data would allow effective detection of very shallow water tables, given the contrast with the volcanic layers, which have resistivities above 1,000 Ω·m, since water-saturated layers and confined aquifers have documented resistivity values between 1.5 and 15 Ω·m.

These methods, especially magnetometry, can cover large areas of land, which makes it possible to study geological structures at a regional scale and to delimit the deposits at a broader scale. Their thickness can then be characterized locally with the geoelectric method.

4. Conclusions

From the resistivity and magnetic measurements, their processing and filtering, and the geological framework of the study area, it was possible to carry out a preliminary characterization of the rocks and structures present. High resistivity values can be associated with volcanic units composed of tephra and tuff, as well as with consolidated and unconsolidated pyroclastic conglomerates. This is corroborated by previous studies and field observations, which show recent volcanic activity and the presence of a crystalline basement.

From the apparent magnetic susceptibility, the map at 30 m was the model that most closely matched the geological data of the study area, with susceptibilities ranging from -0.00211 to 0.0025 cgs. Finally, the model obtained by magnetic inversion was compared with the resistivity data obtained by geoelectrics and shown in the tomography, which revealed an inverse correlation between magnetic susceptibility and resistivity. In geophysical prospecting, low magnetic susceptibility coexisting with high electrical resistivity can occur in iron ore deposits dominated by oxidized minerals such as hematite (Fe_2O_3) or goethite (hydrated iron oxides).

Magnetic susceptibility measures how easily a material is magnetized. In these minerals, the magnetic domains cancel each other almost completely, producing a very weak response to the Earth's magnetic field. Electrical resistivity measures a material's opposition to the flow of current, and some massive or altered iron ores lacking metallic sulfides behave as natural insulators.

The electrical inversion, with a maximum modeled depth of 9.5 m, resolves small areas in high detail, but these require further measurements. In comparison, the magnetic inversion, which reached depths of 900 m, supports a more panoramic, territorial study. This suggests that the two methods can be combined: first the magnetic method over the entire area, followed by the more precise electrical method over selected targets.

5. Acknowledgements

The authors thank the Universidad Distrital Francisco José de Caldas, particularly to its topography laboratory, for providing the GPS equipment and the ABEM SAS Terrameter owned by the university.

6. Author contributions

Luis Miguel Fernández Ricardo: data acquisition, investigation, formal analysis, validation, visualization, software, and writing (original draft).
Alejandro Herrera Tovar: data acquisition, investigation, validation, visualization, software, and writing (original draft).
Robinson Quintana Puentes: investigation, conceptualization, formal analysis, methodology, supervision, writing (original draft; review and editing).

7. Funding

This research received no external funding.

8. Data availability

The data supporting the findings of this study are available from the corresponding author upon request.

9. Conflict of interest

The authors declare that they have no known competing financial interests or personal relationships that could have appeared to influence the work reported in this paper.

10. Use of artificial intelligence

During this work, the authors did not employ any technologies associated with artificial intelligence.

References

[1] Grupo Socio Ambiental, "Exploración," Agencia Nacional de Minería (ANM), 2014. [Online]. Available: https://www.anm.gov.co/sites/default/files/DocumentosAnm/exploracion.pdf

[2] Grupo Socio Ambiental, "Guía minero ambiental de explotación," Agencia Nacional de Minería (ANM), 2023. [Online]. Available: https://acmineria.com.co/wp-content/uploads/2024/01/Guia_Minero_Ambiental_de_Explotacion.pdf

[3] K. Watson et al., "Application of geophysical techniques to minerals-related environmental problems," U.S. Geological Survey, Reston, VA, USA, Open-File Rep. 01-458, 2001. [Online]. Available: https://pubs.usgs.gov/of/2001/ofr-01-0458/ofr-01-0458.pdf

[4] T. A. Adagunodo, L. A. Sunmonu, and A. A. Adeniji, "An overview of magnetic method in mineral exploration," *J. Glob. Ecol. Environ.*, vol. 3, no. 1, pp. 13–28, 2015. [Online]. Available: http://ir.bowen.edu.ng:8080/bitstream/123456789/999/1/Adagunodo%20et%20al%2c%20%282015%29.pdf

[5] C. G. Xie, N. Reinecke, M. S. Beck, D. Mewes, and R. A. Williams, "Electrical tomography techniques for process engineering applications," *Chem. Eng. J. Biochem. Eng. J.*, vol. 56, no. 3, pp. 127–133, Feb. 1995. https://doi.org/10.1016/0923-0467(94)02907-5

[6] R. Manrique, "Caracterización del estado actual de la minería en el municipio de Paipa (Boyacá) y su relación con el Distrito de Manejo Integrado (DMI) Sochagota," Undergraduate thesis, Environmental Engineering, Universidad Nacional Abierta y a Distancia, Colombia, 2020. [Online]. Available: https://repository.unad.edu.co/bitstream/handle/10596/36852/ramanriquea.pdf?sequence=3&isAllowed=y

[7] M. Bayter et al., "Determinación de minerales estratégicos," Agencia Nacional de Minería (ANM), Grupo de Promoción, 2023. [Online]. Available: https://www.anm.gov.co/sites/default/files/Documento_Determinacio%CC%81n_de_Minerales_Estrate%CC%81gicos.pdf

[8] S. Suárez, "Zonificación Ambiental para la Planificación de la Operación Minera en el Departamento de Boyacá," M.S. thesis, Environmental Engineering, Universidad Pedagógica y Tecnológica de Colombia, Colombia, 2018. [Online]. Available: https://repositorio.uptc.edu.co/server/api/core/bitstreams/9e6d76d7-5466-4e6c-967e-1ace35fb6482/content

[9] G. Renzoni and H. Rosas, "Geological map of Colombia, Sheet 171 (Duitama)," Ingeominas, Bogotá, Colombia, 1997. [Online]. Available: https://www2.sgc.gov.co/MGC/Paginas/mgc_1_5M2023.aspx

[10] S. R. Manosalva and W. E. Naranjo, "Caracterización metalográfica de las manifestaciones de mineral de hierro, Paipa (Boyacá, Colombia)," *Bol. Cienc. Tierra*, no. 20, pp. 89–100, Jun. 2007. [Online]. Available: https://repositorio.unal.edu.co/handle/unal/22223

[11] Gómez, J. & Montes, N.E., compilers. 2020. Geological Map of Colombia 2020. Scale 1:1 000 000. Servicio Geológico Colombiano, Colombia, 2020. https://www2.sgc.gov.co/MGC/Paginas/gmc_1M2020.aspx

[12] G. Hernández-R., "Geología, análisis petrográfico y químico de las rocas volcánicas del sur-oriente de Paipa, Boyacá-Colombia," M.S. thesis, Geology, Universidad Nacional de Colombia, Colombia, 1990.

[13] I. M. Ibraheem, H. Aladad, M. F. Alnaser, and R. Stephenson, "IAS: A new novel phase-based filter for detection of unexploded ordnances," *Remote Sens.*, vol. 13, no. 21, art. no. 4345, Oct. 2021. https://doi.org/10.3390/rs13214345

[14] M. H. Loke and R. D. Barker, "Rapid least-squares inversion of apparent resistivity pseudosections by a quasi-Newton method," *Geophys. Prospect.*, vol. 44, no. 1, pp. 131–152, Jan. 1996. https://doi.org/10.1111/j.1365-2478.1996.tb00142.x

[15] U.S. Geological Survey (USGS), "Gravity/magnetic modeling software," 2004. [Online]. Available: https://www.usgs.gov/products/software

[16] Seequent Ltd., "Oasis montaj: Geosoft core software platform," 2024. [Online]. Available: https://www.seequent.com/es/ayuda-apoyo/guias-y-tutoriales/

[17] L. Medina-N., "Modelo de fuentes de anomalías Geomagnéticas de Campo Total asociadas al estado de la cámara magmática del volcán Galeras, Pasto, Colombia," M.S. thesis, Geophysics, Universidad Nacional de Colombia, Colombia, 2012. [Online]. Available: https://repositorio.unal.edu.co/handle/unal/75128

[18] Geotomo Software, "RES2DINV ver. 3.59: Rapid 2-D resistivity & IP inversion using the least-squares method," 2010. [Online]. Available: http://epsc.wustl.edu/~epsc454/instruction-sheets/Res2dinv03.59.pdf

[19] B. V. de la Torre González, "Definición de zonas de fracturamiento empleando tomografía de resistividad eléctrica 3D," B. S. thesis, Geophysical Engineering, Universidad Nacional Autónoma de México, Mexico, 2010. [Online]. Available: https://ru.dgb.unam.mx/handle/20.500.14330/TES01000653915

[20] N. O. Mariita, "The magnetic method," Kenya Electricity Generating Company Ltd. (KenGen), Kenya, 2007. [Online]. Available: https://rafhladan.is/server/api/core/bitstreams/5cbf2348-ab68-4f07-935c-316635e50dc6/content

[21] T. Garzón G., "Geoquímica y potencial minero asociado a los cuerpos volcánicos en la región de Paipa, Departamento de Boyacá, Colombia." Maestría en Geología, Universidad Nacional de Colombia, Bogotá, 2003.

[22] M. Moreno A., "Caracterización de un sitio contaminado por hidrocarburos usando tomografía de resistividad eléctrica," B.S. thesis, Geophysical Engineering, Facultad de Ingeniería, Universidad Nacional Autónoma de México, Mexico, 2010. [Online]. Available: http://132.248.52.100:8080/xmlui/handle/132.248.52.100/1289

Authors and biographies

Luis Miguel Fernández Ricardo: Cadastral and Geodetic Engineer from the Universidad Distrital Francisco José de Caldas, Bogotá, Colombia. He studied geology at the Universidad Nacional de Colombia and is pursuing a master's degree in urban and regional planning at the Interdisciplinary Center for Development Studies (CIDER), Universidad de los Andes, Bogotá. He works at the Unidad Administrativa Especial de Catastro de Bogotá. Email: lmfernandezr@unal.edu.co

Alejandro Herrera Tovar: Cadastral and Geodetic Engineer from the Universidad Distrital Francisco José de Caldas, Bogotá, Colombia, with a specialization in appraisal. He is currently property coordinator at MHC Ingeniería y construcción de obras civiles and has worked with geographic information systems (GIS). Email: alejandro.h.t.1987@gmail.com

Robinson Quintana Puentes: Cadastral and Geodetic Engineer from the Universidad Distrital Francisco José de Caldas, Bogotá, Colombia. Master's degree in geophysics and a Ph.D. in geosciences at the Universidad Nacional de Colombia. He has worked in many public and private entities in land-use planning and GIS and has advised the United Nations Development Programme (UNDP), the World Bank, the National Hydrocarbons Agency, the Colombian Geological Survey, the Agustín Codazzi Geographic Institute, and mining and oil-and-energy companies worldwide. He is currently a professor in the Faculty of Environment and Natural Resources of the Universidad Distrital Francisco José de Caldas. Email: rquintanap@udistrital.edu.co

CC BY NC SA